Turbulent Shear Stress Profile in a Horizontal Bubbly Channel Flow

Yuichi Murai*, Yoshihiko Oishi**, Toshio Sasaki**, Yoshiaki Kodama***, Fujio Yamamoto**

*Division of Mechanical Science, Sch. of Eng., Hokkaido University, Sapporo, Japan

**Fiber Amenity Eng. Course, Sch. of Eng., University of Fukui, Fukui, Japan

***National Maritime Research Institute, Mitaka, Japan

1. Introduction

Microbubble drag reduction is nowadays known as a practically applicable technique for industrial applications such for a ship. However, there is still a large gap between theoretical and the experimental approaches. In particular, the theoretical works target mainly on small spherical bubbles because of simplicity in mathematical models while the experimental studies deal with relatively large bubbles considering practical uses. In fact the mechanism itself could be different dependent on bubble size, and this point makes the comprehensive understanding delay. So-called microbubble reduces the turbulent shear stress indeed, however large bubbles also realize a significant drag reduction in well-tuned cases.

In the present paper, three topics on the mechanism of drag reduction are introduced. The first topic is on large bubble drag reduction caused by air-films covering a flat wall. The second topic is on intermediate bubble drag reduction caused by relative motion between two phases in a turbulent boundary layer. The third topic is on “true” microbubble drag reduction using water electrolysis that provides the highest drag reduction per void fraction.

2. Drag reduction by large bubbles

In the case of large bubbles, the drag reduction occurs with air films sliding on the target surface. The drag reduction ratio is obtained generally in proportion to the wall-covering area of bubbles (Katsui *et al*. 2003, Latorre *et al*. 2003) . Even though the air film does not have sufficient wide area, certain reduction is obtained. In order to grasp the bubble size dependency in a wide condition, we have carried out direct measurement of wall shear stress using a shear transducer. Fig.1 shows the experimental set up. The test channel is 10mm in height, 100mm in width, and 6000mm in length. Water and air are used as two phases at laboratory temperature. Fig.2 shows typical bubble distributions in three cases of bubble size varying with the speed of water flow.

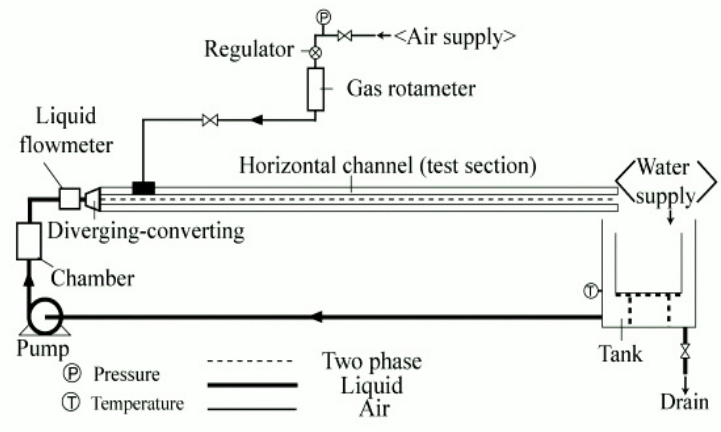

Fig.1 Experimental setup

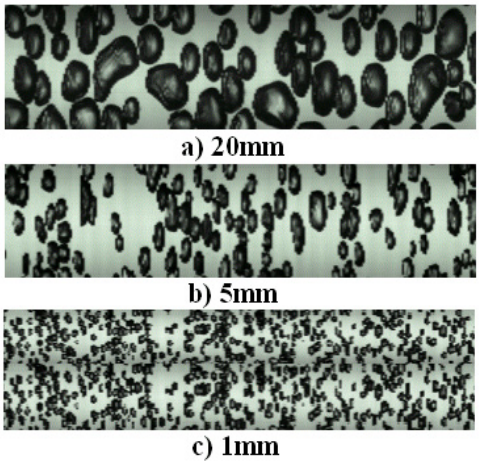

Fig.2 Bubble distribution (top view)

Fig.2 shows the measurement results of friction coefficient ratio from 0 to 20% in bulk void fraction in the channel. The friction coefficient is defined by the directly measured wall shear stress divided by the dynamic pressure of bubbly mixture. In this definition, the mean density reduction by injecting bubbles does not affect the friction coefficient if the structure of boundary layer is kept. In other words, the friction coefficient here can vary only if the structural change occurs in the boundary layer. The measured friction increases initially with the void fraction and begins to reduce at a high void fraction condition. The data also indicate that the friction coefficient is reduced by increment of the mean liquid velocity – as known by past studies (Madavan *et al*. 1985, Merkle & Deutsch 1992)

Fig.3 shows measurement plots of friction coefficient ratio versus mean bubble diameter. Here d* is dimensionless diameter normalized with the channel half height h. The data indicate that the dependency on d* is remarkable in the upstream location (x/h=50 from the bubble generator). The friction becomes maximum value at around d*=1. This implies that the friction tends to decrease in the case of small bubble (d*<1) or in the case of large bubble (d*>1). However, the bubble-size dependency is confirmed no longer in the downstream location (x/h=200) similarly to the results by Kato *et al.* (1999), expressing that the drag modification by relatively large bubbles happens as one of transient phenomena during the development of two-phase boundary layer (Ferrante & Elghobashi, 2004). This result supports the fact that the friction gradually recovers along the streamwise coordinate in channels and for ships, for which relatively large bubbles are mixed in the flow (Kodama *et al*. 2000).

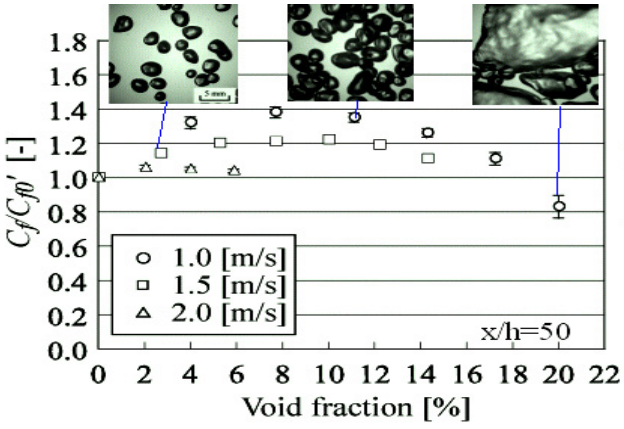

Fig.2 Friction coefficient ratio

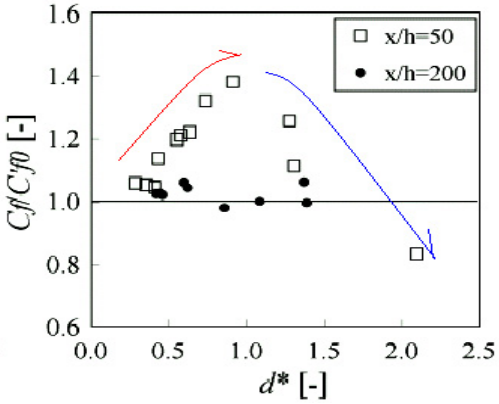

Fig.3 Dependency on bubble diameter

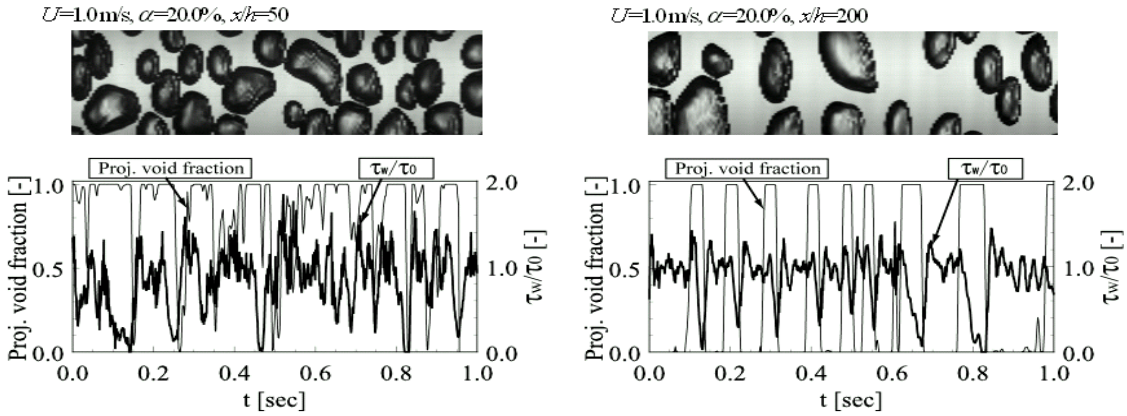

a) Upstream location at x/h=50 b) Downstream location x/h=200

Fig.4 Synchronized measurement of bubble interface and local wall shear stress

Fig.4 shows synchronized measurement result of the local wall shear stress τ_w and local projection void fraction denoted by β. The shear stress tends to decrease in the period of β=1. By careful comparison, we can see that it gradually decreases from the front to the rear part of the period. Thus, the friction is more sensitively reduced in the rear part of individual bubble. This fact leads to an idea that there is a secondary flow in the rear part of bubbles sliding on the wall. This is one of sliced views of the drag reduction mechanism obtained by large bubbles.

3. Drag reduction by intermediate bubbles

In the case of intermediate bubble size with the order of 1mm, a complex translational motion of bubbles relative to the liquid flow begins to appear. This motion is governed by well-known seven force components of bubbles, and is also affected by significant deformation. The drag reduction mechanism in such a case should be investigated by measuring the spatio-temporally resolved flow field in the boundary layer. For this topic, there are a number of reports published until today such as by Gabillet *et al*. (2002), and Kitagawa *et al.* (2003). Our aim is to clarify the drag modification mechanism using data analysis as two-phase flow.

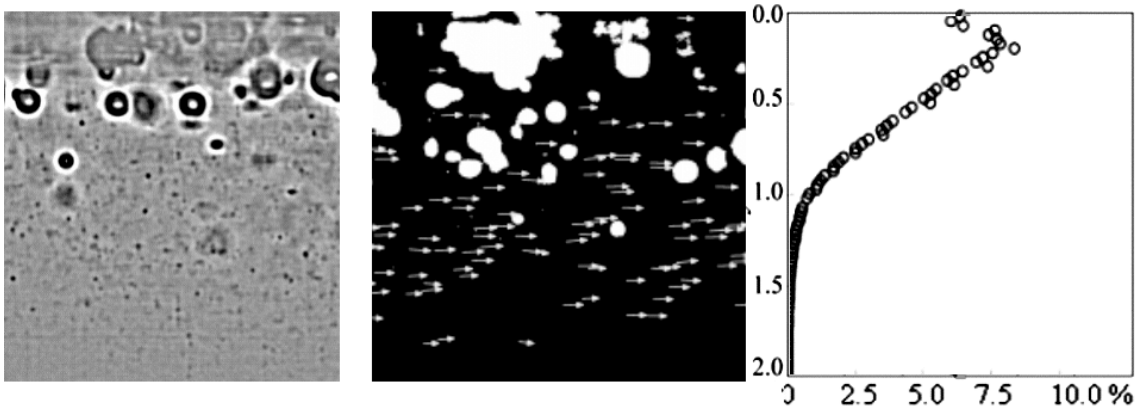

a) original image b) velocity vectors by PTV c) mean void fraction profile

Fig.5 Measurement of two-phase structure using particle tracking velocimetry

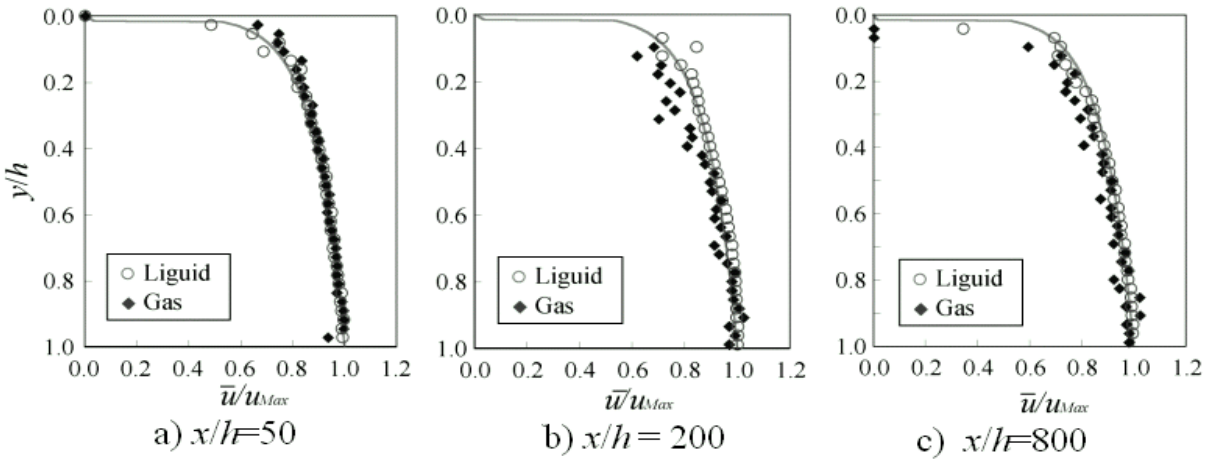

Fig.6 Mean velocity profiles of two phases at three locations

Fig.5 represents a) a sample of original image obtained by high speed video camera at 4000 fps, b) the velocity vectors of tracer particles obtained by particle tracking velocimetry (PTV), and c) mean void

fraction obtained by binarizing the image. Fig.6 shows the mean velocity profiles at the top half channel. The bubbles tend to move with a slightly slower velocity than the liquid, which approximately follows 1/7th power law from the channel wall.

Using the PTV data, the following turbulent shear stress profile is calculated.

$$\tau = \mu\frac{\partial\bar{u}}{\partial y} - \rho\left(1-\bar{\alpha}\right)\overline{u'v'} + \rho\bar{u}\overline{\alpha'v'} + \rho\overline{\alpha'u'v'} \tag{1}$$

This is derived from the momentum conservation equation of bubbly two-phase mixture by Reynolds averaging technique. The turbulent shear stress consists of viscous shear stress (1st term), Reynolds shear stress (2nd term), vertical correlation stress (3rd term), and triple correlation stress (4th term). Here, α, u, and v are basic variable averaged with a control volume. Fig.7 shows the measurement data of the shear stress profile. Noted that the measurement accuracy in the vicinity of the wall is not sufficient because of the optical limitation of PTV. This limitation usually underestimates the correlation in this layer since random error always leads to smaller correlation of two variables. The data have shown that the correlation α'v' had a negative stress in the upper half of the channel contributing to the drag reduction though α'u'v' generated positive stress. It is also confirmed that increasing control volume for the volume averaging weakens these correlations. The mechanism of producing negative value for the vertical correlation stress relates to the fact that there is a vertically oscillating motion of bubbles in the boundary layer. The balance among added inertia, lift, and buoyancy acting on individual bubble induces the oscillation. For instance, the bubbles reached up near the wall surface receive a strong lift force that pushes back downward due to the streamwise slip velocity, and the bubbles suspended far from the wall rise up for the buoyancy. According to our observation, the oscillation was around 100Hz in frequency and 20mm in wavelength in the streamwise direction. We are now analyzing the motion of oscillating bubbles and the correlation to the turbulence events of liquid phase. This point is probably a major mechanism of the drag reduction accompanied with intermediate bubbles.

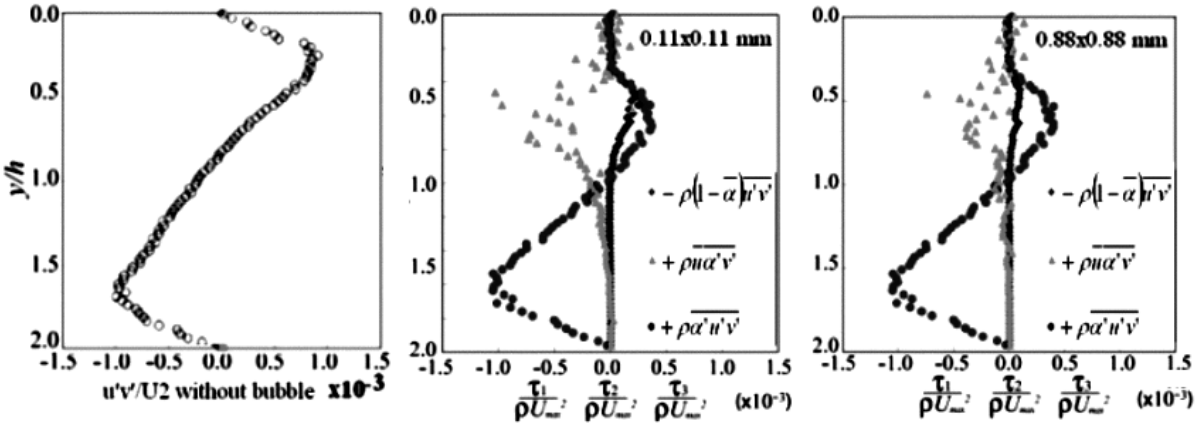

a) single-phase Reynolds shear b) two-phase /fine grid c) two-phase /rough grid

Fig.7 Three kinds of turbulent shear stresses in two-phase channel flow

4. Drag reduction by microbubbles

The most remarkable drag reduction was obtained by means of so-called microbubbles less than 0.2mm in average diameter (McCormick & Bhattacharyya, 1973) . Gravity no longer governs the flow structure in such a case, and there is no deformation of bubbles. In the past studies, a high-speed microbubble flow faster than 5m/s has been investigated (Hassan, 2004). In the present report, microbubble channel flow at a

low speed flow less than 2m/s is tested. The method of bubble generation employed here is water electrolysis. The initial design of the electrodes was an arrangement of thin cylinders as shown in Fig.8 a). This type disturbs and reduces the flow inside the boundary layer apparently, and the measurement result of the wall shear stress was too small. We think that the microbubble drag reduction experiment using electrolysis based on wire-type electrodes – done in the other institute – involves significant effect of the flow disturbance which should be separated from the microbubble effect. Therefore, we revised the electrode's form so as to coincide with the wall surface completely as shown in Fig.8 b). The boundary layer flow is visualized using a mirror submerged into the channel at 45 degree to the wall surface as shown in Fig.8 c).

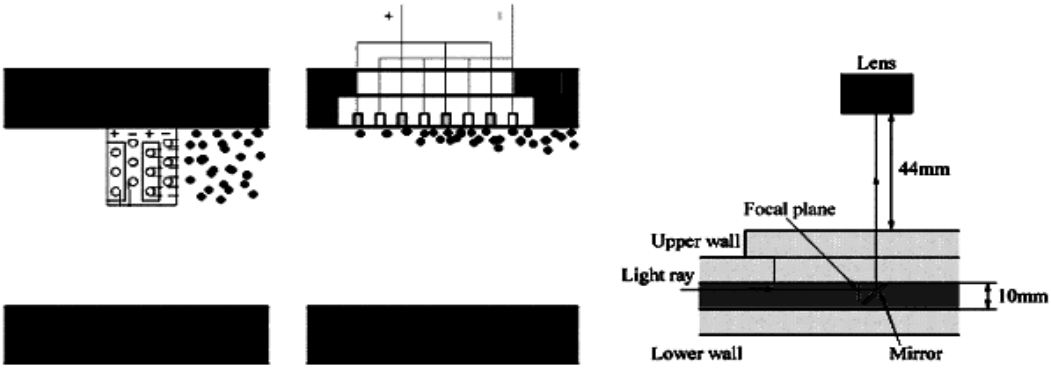

a) cylinder type b) flat type c) optics for visualization

Fig.8 Bubble generator using water electrolysis

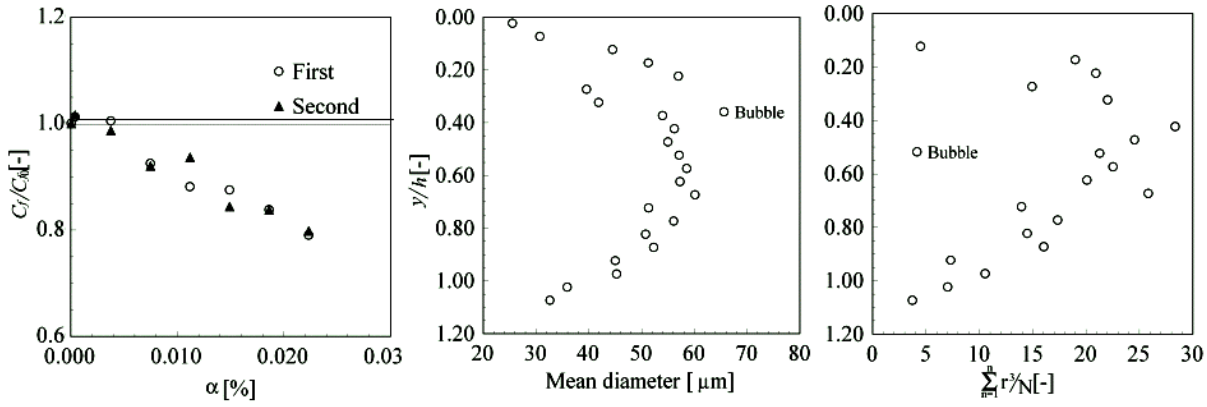

a) friction coefficient ratio b) mean diameter profile c) cubic-mean diameter profile

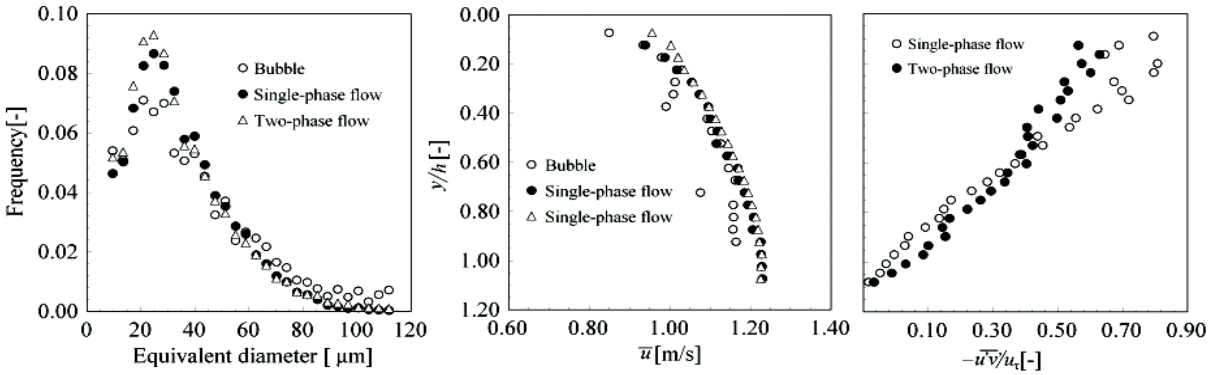

d) histogram of bubble diameter e) mean velocity profile f) Reynolds shear stress

Fig.9 Drag reduction obtained by microbubbles using water electrolysis

Fig.9 shows a set of measurement data of microbubble drag reduction by means of water electrolysis. Electric power used to generate bubbles is 1.2A at 600V. The mean void fraction is exactly estimated by the current using a theory of water electrolysis. As shown in a), the drag reduction is attained around 20% only by 0.02% of void fraction. The sensitivity of the drag reduction, which is defined by the ratio of drag reduction per void fraction is, is in the order of 10^3, and is much larger than the case of large bubbles. 90% of the bubbles concentrate into the range from 10 to 80 micron in diameter, and the time averaged bubble diameter is large in the central region of the channel while it is small near the wall (see the figure b) and c)). For the measurement of liquid phase, tracer particles are seeded in the flow. However, there is no significant difference in their size as shown in d), and therefore, the two phases cannot be distinguished by any image processing scheme. Assuming that there is no relative velocity between the two phases – in fact the slip is order of 0.001m/s and much smaller than the mean velocity -, microbubbles are considered as liquid tracers as well. Analyzing the motion of tracer particles and microbubbles with PTV, it is found that the mean velocity profile does not have significant difference between single- and two- phase conditions. Despite of this, Reynolds shear stress which is directly measured by PTV is reduced around 20% in the vicinity of wall, and it generally corresponds to the measured percentage of the drag reduction. Therefore, it can be said that the drag reduction by microbubbles is attained with decrease in Reynolds shear stress near the wall (Fukagata *et al*. 2004). The reason why the Reynolds shear stress is reduced remarkably by microbubbles has not been directly ascertained from our measurement. For the so-called microbubbles we think that the drag reduction occurs with attenuation of turbulent coherent structure inside the boundary layer as reported by a number of researchers(e.g. Maxey & Riley 1983, Xu *et al*. 2002, Ferrante & Elghobashi, 2004).

6. Summary

The mechanism of frictional drag reduction using bubbles is discussed in three different cases. According to a series of turbulent channel flow experiments, we have obtained following conclusions. 1) Large bubbles also reduce the wall friction if a large void fraction is provided in the flow. To the contrary, a bubble, which has about the channel half height in diameter, generates the largest wall shear stress. This implies that we need to avoid such a bubble size to raise the efficiency of the drag reduction. 2) The local wall shear stress is reduced in the rear part of individual bubbles in the case of large bubbles. That is to say, the drag reduction effect by use of large bubbles can be estimated by the local liquid flow field between a bubble and a wall surface. 3) There is significant correlation measured for the three terms of two-phase turbulent shear stresses. The vertical correlation stress α'v' has a significant negative value contributing to the drag reduction in the case of intermediate bubble size. This component grows up in the case of 1mm-order-bubble due to its vertical oscillatory motion in the boundary layer. 4) Microbubbles less than 0.1mm in average diameter undoubtedly reduces the drag and its sensitivity reaches up to 10^3. In this experiment, we employed wall-coincided electrodes to avoid flow disturbance by the electrodes. Reynolds shear stress measured by PTV decreases around 20% in the vicinity of the wall only by 0.02% in mean void fraction.

Acknowledgement

The authors of this paper are grateful for the support of the Office of Naval Research under Grant N00014-03-1-0299, Dr.L.Patrick Purtell and also for National Maritime Research Institute of Japan

References

Ferrante, A., Elghobashi, S., 2004, On the physical mechanisms of drag reduction in a spatially developing turbulent boundary layer laden with microbubbles, J. Fluid Mech., 503, pp.345-355

Fukagata, K., Iwamoto, K., Kasag, N., 2002, Contribution of Reynolds stress distribution to the skin friction in wall-bounded flows, Phys. Fluids, 14, pp.73-76

Gabillet, C., Colin, C., Fabre, J., 2002, Experimental study of bubble injection in a turbulent boundary layer, Int. J. Multiphase Flow, 28, pp.553-578

Hassan, Y.A., 2004, Drag reduction by microbubble injection, Proc. 3rd Int. Symp. On Two-phase Flow Modelling and Exp., Pisa, pp.1-6

Kato, H., Iwashina, T., Minyanaga, M., Yamaguchi, H., 1999, Effect of microbubbles on the structure of turbulence in a turbulent boundary layer, J. Mar. Sci. Tech., 4, pp.155-162

Katsui, T., Okamoto, Y., Kasahara, Y., Shimoyama, N., Iwasaki, Y., Soejima, S., Hirayama, A., 2003, A study of air lubrication method to reduce frictional resistance of ship, J. Kansai Soc. N.A., Japan, 239, pp.45-53 (in Japanese)

Kodama, Y., Kakugawa, A., Takahashi, T., Kawashima, H., 2000, Experimental study on microbubbles and their applicability to ships for skin friction reduction, Int. J. Heat and Fluid Flow, 21, pp.582-588

Kitagawa, A., Fujiwara, A., Hishida, K., Kakugawa, A., Kodama, Y., 2003, Turbulence structures of microbubble flow measured by PIV/PTV and LIF techniques, Proc. 4th Symp. on Smart Control of Turbulence, pp.131-140

Latorre, R., Miller, A., Philips, R., 2003, Micro-bubble resistance reduction on a model SES catamaran, Ocean Eng., 30, pp.2297-2309

Legner H.H., 1984, Simple model for gas bubble drag reduction, Phys. Fluids, 27, pp.2788-2790

Madavan N.K., Deutsh S., Merkle, C.L., 1985, Measurement of local skin friction in a microbubble modified turbulent boundary layer, J. Fluid Mech., 156, pp.237-256

Marie, J.L., 1987, A simple analytical formulation for microbubble drag reduction, J. Phys-Chem Hydro. 13, pp.213-220

Maxey, M.R., Riley, J., 1983, Equation of motion for a small rigid sphere in a turbulent fluid flow, Phys. Fluids, 26, pp.883-889

McCormick, M., Bhattacharyya, R., 1973, Drag reduction of a submersible hull by electrolysis, Nav. Engg. J., 85, pp.11-11

Merkle, C.L., Deutsch S., 1992, Microbubble drag reduction in liquid turbulent boundary layers, ASME Appl. Mech. Rev., 45, 3, pp.103-127

Serizawa, A., Kataoka, I., 1990, Turbulence suppression in bubbly two-phase flow, Nucl. Eng. Des., 122, pp.1-16

Xu, J., Maxey, M., Karniadakis, G., 2002, Numerical simulation of turbulent drag reduction using micro-bubbles, J. Fluid Mech., 468, pp.271-281